THE JOURNAL OF BIOLOGICAL CHEMISTRY VOL. 287, NO. 12, pp. 9525–9533, March 16, 2012

Lipid Polarity Is Maintained in Absence of Tight Junctions*

Received for publication, November 23, 2011, and in revised form, January 27, 2012 Published, JBC Papers in Press, January 31, 2012, DOI 10.1074/jbc.M111.327064

Junichi Ikenouchi[‡§1], Mayu Suzuki[‡], Kazuaki Umeda[¶], Kazutaka Ikeda[‖], Ryo Taguchi[‖**], Tetsuyuki Kobayashi[**‡‡], Satoshi B. Sato[§§], Toshihide Kobayashi[¶¶], Donna B. Stolz[‖‖], and Masato Umeda[‡]**

*From the [‡]Department of Synthetic Chemistry and Biological Chemistry, Graduate School of Engineering, Kyoto University, Kyoto 615-8510, Japan, [§]PRESTO, Japan Science and Technology Agency, Saitama 332-0012, the [¶]Department of Molecular Pharmacology, Graduate School of Medical Sciences, Kumamoto University, 1-1-1 Honjo, Kumamoto 860-8556, Japan, the [‖]Department of Metabolome, Graduate School of Medicine, The University of Tokyo, Bunkyo-ku, Tokyo 113-0033, Japan, **CREST, Japan Science and Technology Agency (JST) , Kawaguchi, Saitama 332-0012, Japan, the [‡‡]Department of Biology, Faculty of Science, Ochanomizu University, Tokyo 112-8610, Japan, the [§§]Research Center for Low Temperature and Material Sciences, Kyoto University, Kyoto 606-8501, Japan, [¶¶]RIKEN, Wako, Saitama 351-0198, Japan, and the [‖‖]Department of Cell Biology and Physiology, University of Pittsburgh School of Medicine, Pittsburgh, Pennsylvania 15261*

Background: Tight junctions (TJs) are thought to prevent lipids from diffusing freely between the apical and basolateral membrane.
Results: We demonstrated that lipids from the apical and basolateral membranes are segregated in an epithelial cell line lacking ZO-proteins.
Conclusion: TJs are not essential for the maintenance of lipid polarity in epithelial cells.
Significance: We demonstrated that the formation of TJs and lipid polarity occurs independently in epithelial cells.

The role of tight junctions (TJs) in the establishment and maintenance of lipid polarity in epithelial cells has long been a subject of controversy. We have addressed this issue using lysenin, a toxin derived from earthworms, and an influenza virus labeled with a fluorescent lipid, octadecylrhodamine B (R18). When epithelial cells are stained with lysenin, lysenin selectively binds to their apical membranes. Using an artificial liposome, we demonstrated that lysenin recognizes the membrane domains where sphingomyelins are clustered. Interestingly, lysenin selectively stained the apical membranes of epithelial cells depleted of zonula occludens proteins (ZO-deficient cells), which completely lack TJs. Furthermore, the fluorescent lipid inserted into the apical membrane by fusion with the influenza virus did not diffuse to the lateral membrane in ZO-deficient epithelial cells. This study revealed that sphingomyelin-cluster formation occurs only in the apical membrane and that lipid polarity is maintained even in the absence of TJs.

Epithelial cells are constitutively polarized, allowing them to fulfill several fundamental roles such as the provision of vectorial transport (1). There are two membrane domains of epithelial cells, the apical membrane and basolateral membrane. A number of membrane proteins show asymmetric distribution in the plasma membrane in epithelial cells.

In addition to the asymmetric distribution of membrane proteins, several groups have reported lipid asymmetry in epithelial cells. Mostov and co-workers (2, 3) recently showed that phosphatidylinositol 3,4,5-trisphosphate is enriched in the basolateral membrane, and phosphatidylinositol 4,5-bisphosphate is accumulated in the apical membrane, based on their experiments using phosphatidylinositol-binding pleckstrin-homology domains fused with GFP. On the other hand, the ratio of sphingomyelin/phosphatidylcholine was reported to be higher in the apical membrane than the basolateral membrane, based on biochemical experiments using two types of envelope viruses (4).

This raises an important question; How is such lipid polarity maintained within continuous membranes in epithelial cells? TJs[2] are thought to function as the diffusion barrier against membrane lipids and to play essential roles in epithelial polarity by maintaining the asymmetric distribution of lipids (5, 6). TJs are one of the constituents of the epithelial junctional complex and are particularly concentrated at its apex. Three closely related MAGUKs (membrane-associated guanylate kinase-like homologues), ZO-1/ZO-2/ZO-3, make up the undercoat structure of TJs (7, 8). As constituents of TJs themselves, integral membrane proteins such as claudins, occludin, tricellulin, and junctional adhesion molecules (JAMs) have been identified (9, 10). To better define the roles of TJs in epithelial polarity, ZO-1/ZO-2/ZO-3-deficient epithelial cells (ZO-deficient cells) were recently established by Tsukita and co-workers (11). In ZO-deficient cells, the formation of belt-like adherens junctions was significantly delayed during epithelial polarization, but once formed, the belt-like adherens junctions were normal (12, 13). On the other hand, ZO-deficient cells lacked TJs completely (11, 12). Claudins were not concentrated at cell-cell contacts, and TJ strands were never observed in ZO-deficient cells.

* This work was supported by grants from the Ministry of Education, Culture, Sports, Science, and Technology of Japan (to M. U. and J. I.) and from the Precursory Research for Embryonic Science and Technology, Japan Science and Technology Agency (to J. I.).
[1] To whom correspondence should be addressed. Tel.: 81-75-383-2768; Fax: 81-75-383-2767; E-mail: ikenouchi@sbchem.kyoto-u.ac.jp.

[2] The abbreviations used are: TJ, tight junction; DOPC, 1,2-di-oleoyl-*sn*-glycero-3-phosphocholine; DOPE, 1,2-dioleoyl-*sn*-glycero-3-phosphoethanolamine; SM, sphingomyelin; NBD, nitrobenzoxadiazole; RFP, red fluorescent protein; ZO, zonula occludens; CB, coating buffer; R18, octadecylrhodamine B; PC, phosphatidylcholine; GUV, giant unilamellar vesicle; PS, phosphatidylserine.

Surprisingly, the asymmetric distribution of membrane proteins was normal in ZO-deficient epithelial cells, indicating that TJs are dispensable for asymmetric distribution of membrane proteins. Clevers and co-workers (14) also reported that the activation of LKB1 induced epithelial polarization in a cell-autonomous fashion in single cells and that TJs are not necessary for the asymmetric distribution of membrane proteins. However, the roles of TJs in lipid asymmetry remain unclear.

In this study we used a sphingomyelin-specific probe, lysenin, that is a toxin from earthworms and showed for the first time that sphingomyelin is clustered only in the apical membrane of epithelial cells. Furthermore, we clearly demonstrated that the apical polarization of sphingomyelin clusters occur in the absence of TJs and TJs are not the lateral diffusion barrier of lipids in epithelial cells.

EXPERIMENTAL PROCEDURES

Cells and Cell Culture—EpH4 cells (generously provided by Dr. E. Reichmann, Institute Suisse de Recherches, Lausanne, Switzerland) and MTD1A cells were grown in Dulbecco's modified Eagle's medium supplemented with 10% fetal calf serum. The Ca^{2+} switch assay was performed as previously described (15).

Immunofluorescence Microscopy—Cells cultured on coverslips were fixed with 1% paraformaldehyde for 5 min. After washing with PBS containing 0.9 mM $CaCl_2$ and 0.5 mM $MgCl_2$ (PBS+), cells were treated with 50 μg/ml digitonin for 10 min on ice for permeabilization. The permeabilized cells were incubated with 1 μg/ml GFP-tagged or RFP-tagged lysenin at 4 °C on ice for 10 min. After washing with PBS+, cells were fixed with 2% paraformaldehyde for 10 min on ice. This second fixation was necessary to immobilize lysenin and prevent artificial aggregation. Blocking was done by incubating the fixed cells with 5% BSA in PBS for 10 min at room temperature. After the antibodies had been diluted with the blocking solution, the cells were incubated at room temperature for 1 h with the primary antibody and then for 30 min with the secondary antibody. The procedure of double immunofluorescence microscopy was as described previously (15).

Fluorescence Recovery after Photobleaching Analysis—Cells were plated onto glass-base dishes (Iwaki Glass, Tokyo, Japan) and grown to confluency. After incubation with the R18-labeled influenza virus at 4 °C for 30 min, cells were treated with PBS-citrate containing 1 mM $CaCl_2$ and 0.5 mM $MgCl_2$, pH 5.0, to induce viral fusion. R18-labeled cells were subjected to fluorescence recovery after photobleaching by using a FluoView 500 confocal laser scanning microscope (Olympus, Melville, NY) equipped with a He-Ne laser (543 nm). Briefly, an apical membrane region was chosen, and an image was captured. The selected region of interest was then bleached (100% power) for $<$1 min and allowed to recover for 450 s. Imaging during this time occurred at 8-s intervals at low power (50%). Raw data were first adjusted by background subtraction at each time point, corrected to three independent regions that had not been photobleached, and then normalized to the background-subtracted prebleach image. Kinetic modeling was performed using Prism software (Graphpad Software, San Diego, CA) to obtain the mobile fraction value.

Scanning Electron Microscopy—The isolated apical and basolateral membranes on cover glasses were prepared for scanning electron microscopy by fixing them with a solution of 1% paraformaldehyde, 1% glutaraldehyde, 100 mM KCl, 20 mM HEPES, 5 mM $MgCl_2$, and 1 mM $CaCl_2$ at pH 6.8 for 30 min. The apical membranes were allowed to settle onto Cell-Tak (BD Biosciences)-coated cover glasses at 1*g* for 1 h, then fixed as described above. Samples were washed 4 times with water and post-fixed in 0.22-μm filtered 1% osmium tetroxide in 100 mM sodium cacodylate, pH 7.0, for 30 min. The preparations were washed several times in a graded series of solutions (10, 20, 30, 40%, 50, 60, 70, 80, 90, and 95 and 4× in 100%) for 10 min per step. Samples were critical point-dried, sputter-coated (Polaron E5000 sputter coater; Polaron Equipment, Watford, UK), and viewed on a JSM 6335F scanning electron microscope (JEOL, Tokyo, Japan) at 5 kV.

Expression Vectors—The cDNA encoding lysenin (161–298 amino acids) was amplified by PCR, supplemented with enhanced GFP or monomeric red fluorescent protein tag, and ligated into pRSET vector as described previously (16). His-enhanced GFP or monomeric red fluorescent protein-lysenin(161–298) was expressed in *Escherichia coli*, and purified by affinity chromatography using TALON metal affinity resin (Clontech, Palo Alto, CA).

Myc-tagged PATJ expression vector was kindly provided by Dr. M. Adachi (Kyoto University) (17). cDNA of mouse Par-6 was amplified by RT-PCR using the cDNA library of EpH4 cells as a template. The amplified fragment was subcloned into the pCAGGS-nMyc vector.

The shRNA oligonucleotide sequence against mouse Par-6 was 5′-CCAGCGTAATAATGTGGTA-3′. The shRNA oligonucleotide sequence against mouse PATJ was 5′-GAGACGAGCTGCTAGAGAT-3′. Double-stranded oligos were cloned into the H1 promoter vector.

Preparation of Giant Unilamellar Vesicles (GUVs)—Giant liposomes were made from hybrid films of agarose and lipids according to a modified version of the method of Horger *et al.* (18).

Antibodies and Fluorescence-labeled Lipids—Rabbit anti-claudin-3 polyclonal antibody was purchased from Zymed Laboratories Inc. (San Francisco, CA). Rat anti-E-cadherin mAb (ECCD2) was purchased from Takara (Tokyo, Japan). Mouse anti-GM130 mAb and anti-Grp78/Bip were purchased from BD Transduction Laboratories. Mouse anti-FLAG mAb (M2) was purchased from Sigma. Rabbit anti-ZO-2 polyclonal antibody was purchased from Santa Cruz Biotechnology (Santa Cruz, CA). Rabbit anti-syntaxin 3 was purchased from Synaptic Systems (Gottingen, Germany).

The DOPC (1,2-di-oleoyl-sn-glycero-3-phosphocholine), sphingomyelin (d18:1–16:0) *N*-palmitoyl-D-*erythro*-sphingosylphosphorylcholine), cholesterol, rhodamine-DOPE (1,2-dioleoyl-*sn*-glycero-3-phosphoethanolamine-*n*-(lissamine rhodamine B sulfonyl)), C12-NBD-sphingomyelin (*N*-[12-[(7-nitro-2–1,3-benzoxadiazol-4-yl)amino]lauroyl]-sphingosine-1-phosphocholine), and 18:1– 06:0 NBD PS 1-oleoyl-2-{6-[(7-nitro-2–1,3-benzoxadiazol-4-yl)amino]hexanoyl}-*sn*-glycero-3-phosphoserine were obtained from Avanti Polar Lipids

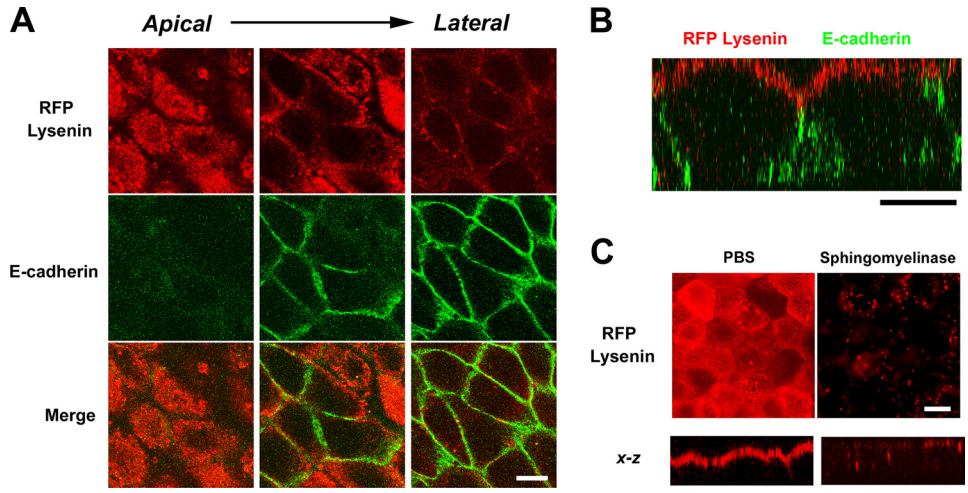

FIGURE 1. **Selective recognition of the apical membrane of epithelial cells by lysenin.** *A*, EpH4 cells were fixed and stained with RFP-lysenin (*red*) and anti-E-cadherin mAb (*green*) (*scale bar*, 10 μm). *B*, *xz* section of a confocal image demonstrates that lysenin selectively recognized the apical membrane (*scale bar*, 10 μm). *C*, cells were treated with bacterial sphingomyelinase before fixation for 15 min at 37 °C. In bacterial sphingomyelinase-treated cells, staining of lysenin in the apical membrane disappeared (*scale bar*, 5 μm).

(Alabaster, AL). Bacterial sphingomyelinase (from *Staphylococcus aureus*) was obtained from Sigma.

Quantitative Measurement of Fluorescence Derived from GFP-lysenin Associated with GUVs—Fluorescent images were analyzed with ImageJ software as described previously (19). The fluorescence signal of GFP-lysenin along GUVs (Y_{circle}) and the fluorescence signal of the external medium (Y_{env}) were measured under the same conditions of microscopy. Then the value of Y_{circle}/Y_{env} was calculated for each GUV.

Isolation of Apical Membrane and Basolateral Membrane of Cultured Epithelial Cells with Colloidal Silica—The apical membrane, basolateral membrane, and internal membrane were isolated using a modified version of the method of Stolz *et al.* (20). In brief, EpH4 cells were washed twice with coating buffer (CB) (135 mM NaCl, 20 mM MES, 1 mM Mg^{2+}, 0.5 mM Ca^{2+}, pH 5.5). Then the cells were coated with a 1% (w/v) cationic colloidal silica solution in CB. After coating, the cells were washed with CB, then coated using a 1 mg/ml polyacrylic acid solution in CB at pH 5.0. The cells were washed again with CB. Using a 5-ml syringe fitted with a flattened 18-gauge needle, shear forces were applied to the cells by squirting them with CB containing protease inhibitor mixture (Nacalai Tesque, Kyoto, Japan). Complete cell lysis was confirmed by observation under the light microscope. The basolateral membrane domains remained on the dish. The lysate solution was mixed with the same amount of 100% (w/v) Nycodenz in CB and sedimented through a cushion of 85% (w/v) Nycodenz in CB. The dense silica-coated apical membrane was obtained by centrifugation at 100,000 × *g* as a pellet. The floating fraction was obtained as the 100,000 × *g* supernatant.

Mass Spectrometric Analysis of Lipids—After Bligh and Dyer extraction of lipids from the apical membrane and basolateral membrane of epithelial cells, the extracted lipids were subjected to mass spectrometric analysis using the electrospray ionization-MS/MS system described in Taguchi *et al.* (21).

R18-labeled Influenza Virus—Influenza A virus (*A/PR 8/34*) isolated from eggs was kindly provided by Dr. M Yamashita (Daiichi Sankyo Co., Ltd). R18 labeling was performed as previously described (22). The cells were incubated with R18-labeled influenza virus at 4 °C for 30 min, then treated with PBS-citrate containing 1 mM $CaCl_2$ and 0.5 mM $MgCl_2$, pH 5.0, to induce viral fusion.

RESULTS

Lysenin Staining Reveals Polarized Distribution of Sphingomyelin in Epithelial Cells—As a tool for visualization of the distribution of sphingomyelin in the cellular membrane, we previously characterized lysenin as a toxin that specifically bound to sphingomyelin (23, 24). In this study, to visualize the distribution of sphingomyelin in epithelial cells, we stained cultured epithelial cells using lysenin. Interestingly, lysenin specifically stained the apical membrane of cultured EpH4 cells, an epithelial cell line derived from mouse mammary glands (Fig. 1, *A* and *B*). In cultured cells of another epithelial cell line, MTD1A, the apical membranes were selectively stained with lysenin.[3] To confirm that lysenin bound to the apical membrane in a sphingomyelin-dependent manner, we treated epithelial cells with bacterial sphingomyelinase before staining. As expected, the treatment with sphingomyelinase abolished the apical staining of lysenin (Fig. 1*C*). In the following experiments, we tried to clarify why lysenin selectively labeled the apical membrane of EpH4 cells.

There Are No Obvious Differences in Molecular Species of Sphingomyelin between Apical and Basolateral Domains—First, we examined differences in the molecular species of sphingomyelin between the apical membrane and basolateral membrane.

To isolate the membrane fraction of the apical and basolateral membrane, we used colloidal silica particles (20). The strategy used to simultaneously isolate both membranes is outlined in Fig. 2*A*. Briefly, the apical membranes of EpH4 cells were coated with positively charged colloidal silica, and then the cells were disrupted mechanically. The apical membrane coated with colloidal silica was obtained as a pellet after centrifugation.

[3] J. Ikenouchi and M. Umeda, unpublished data.

This strategy enabled us to analyze lipids from isolated membranes, because detergents were not used. Biochemical and morphological criteria were subsequently employed to assess the quality of the isolated membranes. The enrichment and degree of contamination were judged by Western blotting with antibodies against several marker proteins as follows. E-cad-

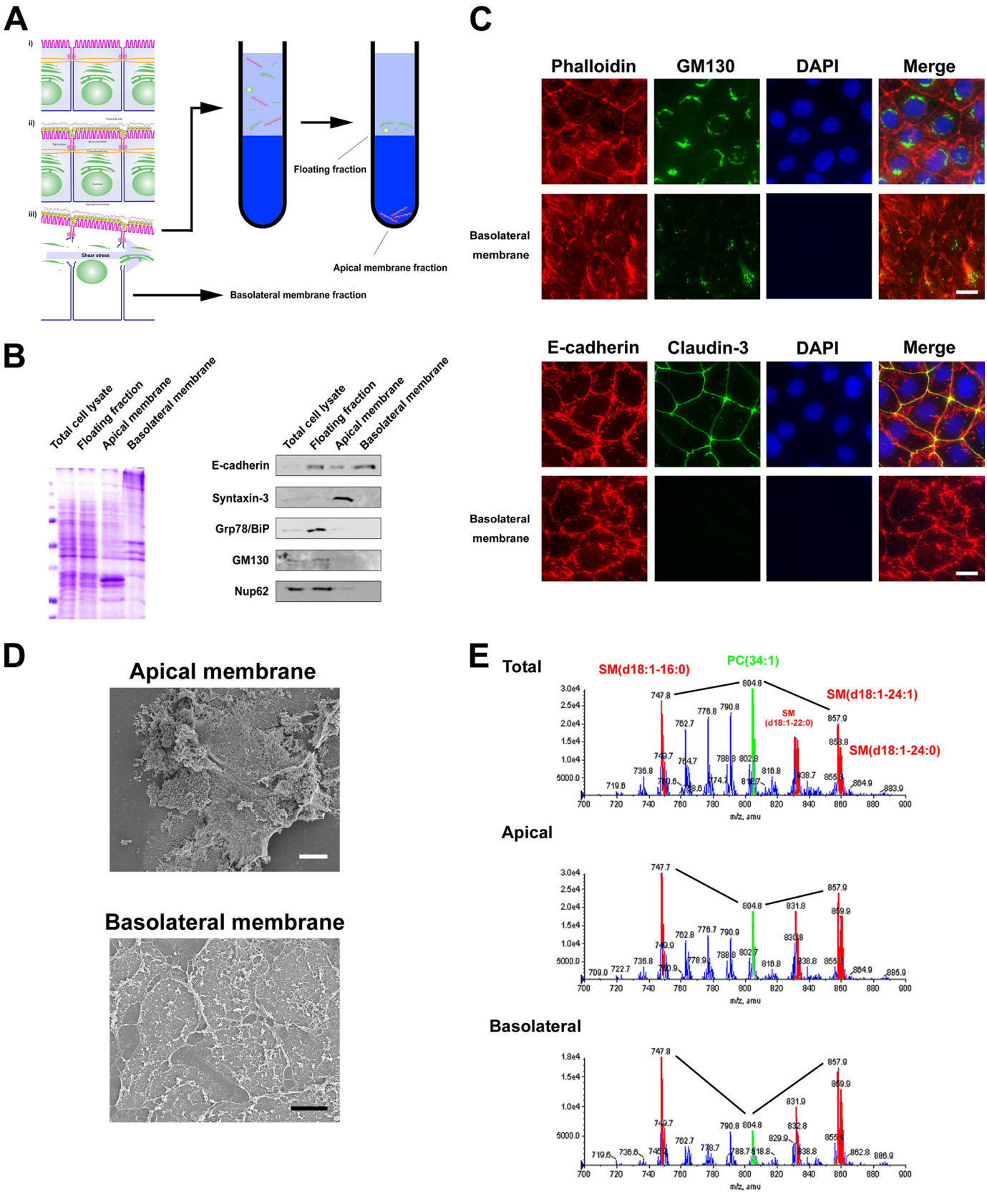

herin was used as a marker for the basolateral membrane protein; syntaxin-3 marked the apical membrane; Grp78/BiP, a HSP70 family member and soluble luminal ER protein, served as a marker for the ER; GM130 was used as a marker for the Golgi membrane; Nup62 was the marker for the nuclear membrane. Immunoblot analyses of the subcellular fractions probed with these antibodies were performed (Fig. 2*B*). The basolateral membrane fraction showed the highest enrichment for E-cadherin. The apical membrane fraction was highly enriched for its marker protein, syntaxin-3, and little contamination of the internal membrane fractions was detectable.

To further assess the purity of the isolated membranes, isolated membranes were fixed and examined by immunofluorescence microscopy and scanning electron microscopy (Fig. 2, *C* and *D*). In the basolateral membrane, the staining of GM130/DAPI/claudin-3 was not observed. Dense cortical actin networks were observed in the apical membrane by scanning electron microscopy (Fig. 2*D*). From these analyses we concluded that the apical membrane fraction and basolateral membrane fraction were obtained with little contamination.

Then lipids were extracted from the apical and basolateral membrane fractions according to the method of Bligh and Dyer. Lipid extracts of these membrane fractions and total cells were then analyzed by electrospray ionization-MS/MS (21). To analyze the contents of sphingomyelin and phosphatidylcholine, the negative ion mode spectra of these membranes were compared (Fig. 2*E*). For peak assignment, each major ion was subjected to product ion scan analysis. There were four major molecular species of sphingomyelin: SM (d18:1–16:0) (*m*/*z* 747.9), SM (d18:1–22:0) (*m*/*z* 831.9), SM (d18:1–24:1) (*m*/*z* 857.9), and SM (d18:1–24:0) (*m*/*z* 859.9). These peaks are colored *red* in the profile (Fig. 2*E*). The molecular species of phosphatidylcholine were PC (alkyl-acyl 32:1) (*m*/*z* 762.8), PC (32:1) (*m*/*z* 776.8), PC (alkyl-acyl 34:1) (*m*/*z* 790.8), PC (34:1) (*m*/*z* 804.8), and PC (alkyl-acyl 36:2) (*m*/*z* 816.8). The peak derived from PC (34:1) is colored *green* in the profile (Fig. 2*E*). All four major sphingomyelin species were present in both the apical and basolateral membrane. PC (34:1) was more abundant than SM (d18:1–16:0) or SM (d18:1–24:1) in the lipid extract of total cells. Intriguingly, sphingomyelin were enriched at the plasma membrane not only in the apical domain but also in the basolateral domain. There were no obvious differences in the relative abundance and the molecular species of sphingomyelin between the apical and basolateral domains.

Sphingomyelin Is Clustered Only in Apical Membranes of Epithelial Cells—We next examined another possibility, *i.e.* that lysenin recognizes other properties of sphingomyelin-containing membranes. Previous studies have shown that the interaction of lysenin and sphingomyelin is affected by the presence of other lipids (23, 24). The mixing of glycosphingolipid and sphingomyelin hinders the formation of clusters of sphingomyelin alone and inhibits the binding of lysenin (24). We have previously shown that sphingomyelin/cholesterol liposomes were 10,000 times more effective than liposomes of sphingomyelin alone in inhibiting lysenin-induced hemolysis (23, 25).

These previous studies led us to examine the distribution of lysenin in artificial GUVs made of various lipid compositions. Previously, it was shown that the cholesterol composition affected the phase transition of sphingomyelin (26). Therefore, we first examined the binding of lysenin to sphingomyelin-rich domains in GUVs of SM (d18:1–16:0)/DOPC/NBD-C12-SM/cholesterol (molar ratio, 27:33:6:33). In GUVs of SM (d18:1–16:0)/DOPC/NBD-C12-SM/cholesterol/rhodamine-DOPE (molar ratio, 27:33:6:33:1), NBD-C12-SM exhibited partitioning complementary to rhodamine-DOPE, indicating that NBD-C12-SM partitions into the ordered-phase domain (Fig. 3*A*). RFP-lysenin was found to bind to the sphingomyelin-rich ordered-phase membranes in GUVs of SM (d18:1–16:0)/DOPC/NBD-C12-SM/cholesterol (molar ratio, 27:33:6:33) (Fig. 3*B*).

Next, the binding of lysenin to GUVs of DOPC/rhodamine-DOPE (molar ratio, 99:1), SM (d18:1–16:0)/DOPC/rhodamine-DOPE (molar ratio, 49:50:1), and SM(d18:1–16:0)/DOPC/cholesterol/rhodamine-DOPE (molar ratio, 33:33:33:1) was examined (Fig. 3*C*). Judging from the uniform distribution of rhodamine-DOPE, the sphingomyelin-rich ordered phase membrane was not formed in GUVs of SM (d18:1–16:0)/DOPC/rhodamine-DOPE (molar ratio, 49:50:1). The fluorescence of GFP-lysenin associated with liposome (Y_{circle}) and the fluorescence of GFP-lysenin outside of the liposome (Y_{env}; environment) were quantitatively measured in each GUV. The value of Y_{circle}/Y_{env} of SM(d18:1- 16:0)/DOPC/cholesterol/rhodamine-DOPE (molar ratio, 33:33:33:1) GUVs was 8.0 $\pm$ 3.2 and significantly higher than that of SM (d18:1–16:0)/DOPC/rhodamine-DOPE (molar ratio, 49:50:1) GUVs (Y_{circle}/Y_{env} = 1.6 $\pm$ 0.1) ($p < 0.05$) (Fig. 3*D*). It is expected that the value of Y_{circle}/Y_{env} of SM/DOPC/cholesterol (1:1:1) GUVs is at most 2.27-fold greater than the value of Y_{circle}/Y_{env} of SM/DOPC (1:1) GUVs if we assume that lysenin binds to sphingomyelin at a constant ratio, considering that the area per sphingomyelin molecule and the area per DOPC molecule are 54.4 and 66.9Å, respectively (27). However, the ratio between them is greater than 2.27, indicating that lysenin binds preferentially to membrane domains in which sphingomyelin is clustered. Considering these results together, we concluded that sphingomyelin

FIGURE 2. **MS profiling of PC and SM molecular species in the apical and basolateral membranes.** *A*, shown is the scheme of apical and basolateral membrane isolation for epithelial cell monolayers cultured in dishes. For details, see "Experimental Procedures." *B*, shown is an immunoblot analysis of the apical membrane fraction, basolateral membrane fraction, and floating fraction. 5 μg of each membrane fraction was separated by SDS-PAGE (Coomassie Brilliant Blue staining in the *left panel*), transferred to nitrocellulose membranes, and probed with antibodies against the indicated marker proteins (*right panel*). The results are representative of three independent experiments. *C*, intact EpH4 cells and basolateral membrane were fixed and stained with the indicated antibodies. Note that signals of GM130/DAPI/claudin-3 were little observed in the basolateral membrane (*scale bar*, 10 μm). *D*, shown is scanning electron micrographs of isolated apical and basolateral membranes (*white bar*, 1 μm; *black bar*, 3 μm). *E*, shown are negative ion mass spectra of the *m*/*z* range 500–1000 of lipid extracts prepared from the apical and basolateral membranes. The peak assignment to sphingomyelin molecular species is indicated (*red*). Compared with the amount of phosphatidylcholine (34:1), sphingomyelin (d18:1–16:0) and sphingomyelin (d18:1–24:1) were enriched in both the apical membrane and basolateral membrane. For additional peak assignments, see "Results." The total carbon chain length (*x*) and number of carbon-carbon double bonds (*y*) of individual lipid molecular species are specified as (*x*:*y*). The results are representative of three independent experiments.

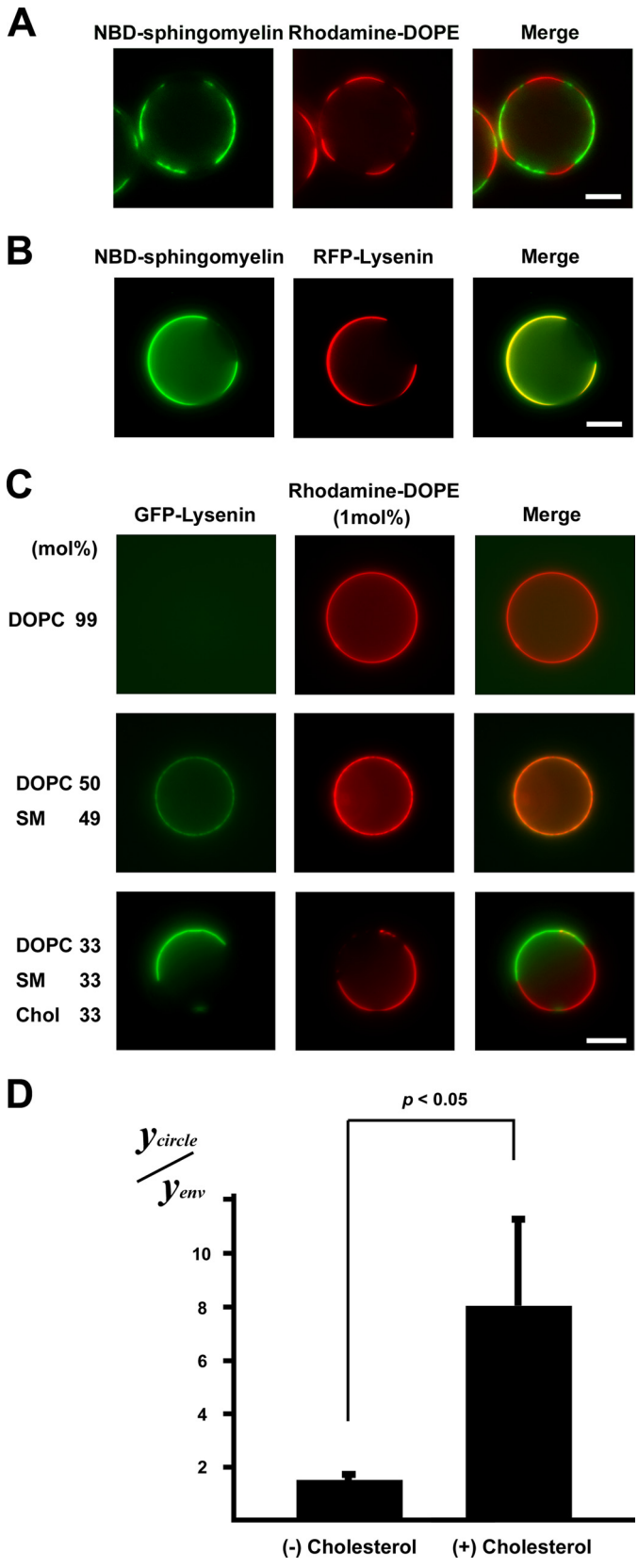

FIGURE 3. **Binding of lysenin to sphingomyelin-containing GUVs.** *A*, shown is the observation of a GUV containing 5 mol% NBD-sphingomyelin (*green*) (NBD-C12-SM/DOPC/SM(d18:1–16:0)/cholesterol 6:33:27:33) and RFP-lysenin (*red*) (*scale bar*, 10 μm). *B*, shown is the observation of binding of GFP-lysenin (*green*) to a GUV of DOPC/rhodamine-DOPE (molar ratio, 99:1) (*upper panel*), SM (d18:1–16:0)/DOPC/rhodamine-DOPE (molar ratio, 49:50:1) (*middle panel*), or SM(d18:1–16:0)/DOPC/cholesterol/rhodamine-DOPE (molar ratio, 33:33:33:1) (*lower panel*). Each GUV contained 1 mol% rhodamine-DOPE (*scale bar*, 10 μm). *C*, the fluorescence of GFP-lysenin associated with liposome ($\boldsymbol{Y}_{circle}$) and the fluorescence of GFP-lysenin outside of the liposome ($\boldsymbol{Y}_{env}$) were quantitatively measured in each GUV. The value of $\boldsymbol{Y}_{circle}/\boldsymbol{Y}_{env}$ of the SM(d18:1- 16:0)/DOPC/cholesterol (*Chol*)/rhodamine-DOPE (molar ratio, 33:33:33:1) and SM (d18:1–16:0)/DOPC/rhodamine-DOPE (molar ratio, 49:50:1) GUVs was calculated. Data are the means ± S.D. of three independent experiments. $p < 0.05$ by Student's *t* test.

was clustered only in the apical membrane of epithelial cells and that sphingomyelin clusters were recognized by lysenin.

Sphingomyelin Clusters Are Formed in Apical Membrane after Formation of Tight Junctions during Epithelial Polarization—We next attempted to determine the time point at which clustering of sphingomyelin occurred during epithelial polarization. The EpH4 cells were cultured in a low Ca^{2+} medium containing 5 μM Ca^{2+} overnight under confluent conditions, and their polarization was initiated by transferring to a normal Ca^{2+} medium (Fig. 4*A*).

At 0.5 h after Ca^{2+} repletion, adherens and tight junctions began to be formed; however, the entire plasma membrane was weakly stained with GFP-lysenin at this time point. At 1.5 h after Ca^{2+} repletion, the formation of adherens and tight junctions was completed in almost all of the EpH4 cells, and the apical membranes of several of the EpH4 cells were stained with GFP-lysenin (Fig. 4*A*). At 6 h after Ca^{2+} repletion, most cells were stained with GFP-lysenin. These observations indicate that the formation of sphingomyelin clusters in the apical membrane occurs after the formation of TJs during epithelial polarization.

Tight Junctions Are Not Required for Establishment and Maintenance of Lipid Polarity—The above results led us to ask how the lipid asymmetry is maintained within continuous membranes in epithelial cells. As TJs are thought to function as the diffusion barrier against membrane proteins and lipids and to play essential roles in epithelial polarity by maintaining the asymmetric distribution of membrane proteins and lipids (5, 6), we examined the distribution of sphingomyelin in the ZO-1/ZO-2/ZO-3-deficient epithelial cells (ZO-deficient cells), which lack TJs completely. As shown previously in ZO-deficient epithelial cells, claudins were not accumulated at the cell-cell boundaries and TJs were not formed (Fig. 4*B*) (11). To test whether TJs are essential for the asymmetric distribution of sphingomyelin clusters at the apical membrane, we stained ZO-deficient cells with GFP-lysenin to visualize the distribution of clustered sphingomyelin. Interestingly, the apical membranes of ZO-deficient cells were also stained with GFP-lysenin, suggesting that sphingomyelin clusters were formed and maintained in the apical membrane even in the absence of TJs (Fig. 4, *C* and *D*). In the Ca^{2+} switch assay, the formation of sphingomyelin clusters in the apical membrane occurred after the formation of circumferential actin rings in ZO-deficient cells (Fig. 4*E*).

Subsequently, we examined the roles of Par-6 and PATJ among epithelial polarity-associated proteins in the formation of sphingomyelin clusters. Overexpression of Par-6 or PATJ and knockdown of PATJ did not affect the formation of sphingomyelin clusters (Fig. 4*F*). On the other hand, knockdown of

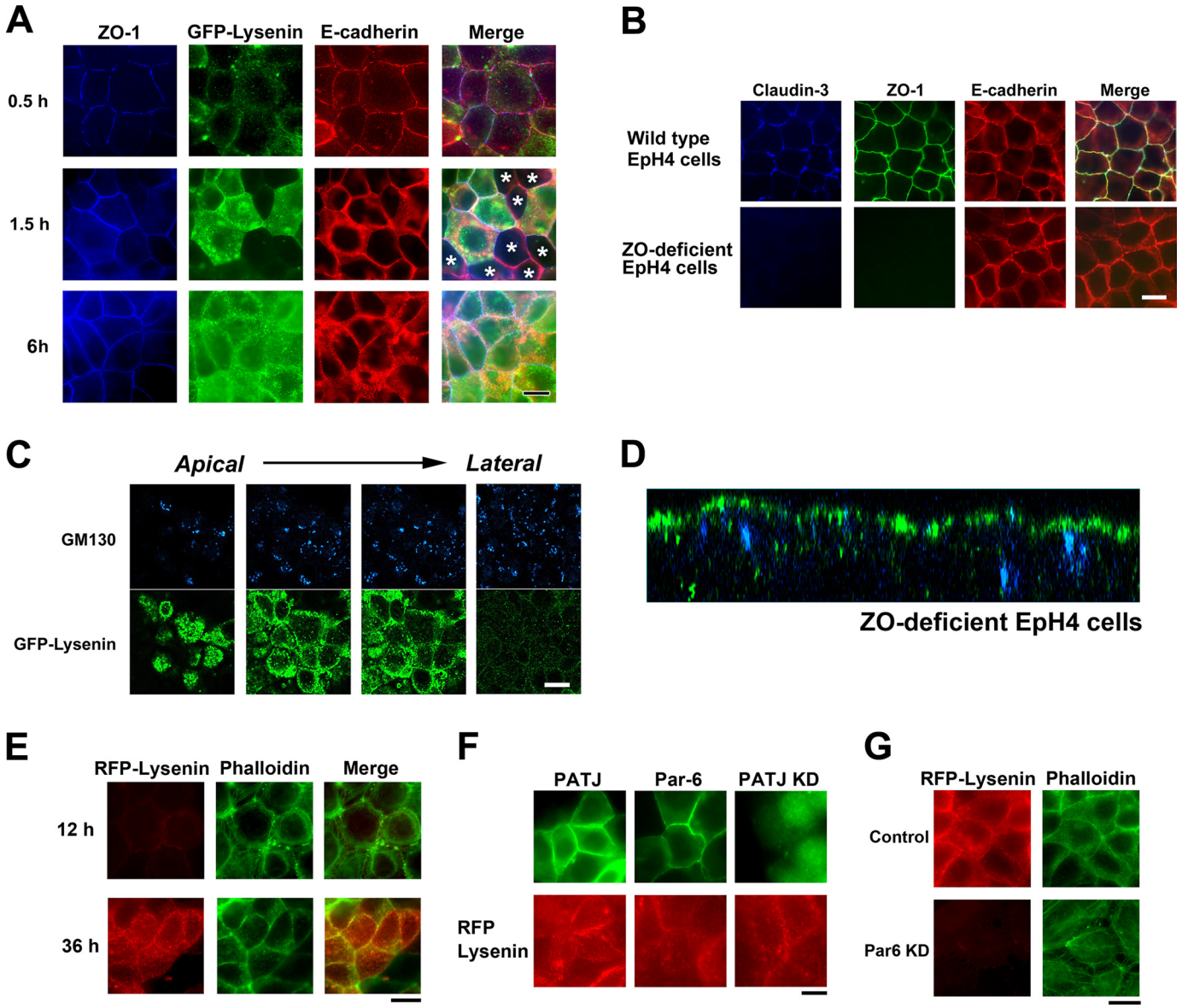

FIGURE 4. **Asymmetric sphingomyelin clusters are retained in the absence of TJs.** *A*, EpH4 cells were cultured overnight in low Ca^{2+} medium, and their polarization was initiated by transferring to normal Ca^{2+} medium. After a 0.5-, 1.5-, or 6-h incubation, cells were fixed and stained with anti-ZO-1 mAb (*blue*), GFP-lysenin (*green*), and anti-E-cadherin mAb (*red*). In some cells TJs were formed based on the staining of ZO-1 before apical sphingomyelin cluster formation (*asterisks*, *middle panel*) (*scale bar*, 10 μm). *B*, EpH4 cells and ZO-deficient EpH4 cells were fixed and stained with anti-claudin-3 polyclonal antibody (*blue*), anti-ZO-1 mAb (*green*), and anti-E-cadherin mAb (*red*) (*scale bar*, 10 μm). *C*, ZO-deficient EpH4 cells were fixed and stained with GFP-lysenin (*green*) and anti-GM130 mAb (*blue*). The asymmetric lysenin staining was maintained in ZO-deficient EpH4 cells (*scale bar*, 10 μm). *D*, *xz* section of a confocal image of *B* is shown. *E*, ZO-deficient cells were cultured in low Ca^{2+} medium overnight, and their polarization was initiated by transferring to normal Ca^{2+} medium. After a 12- or 36-h incubation, cells were fixed and stained with RFP-lysenin (*red*) and phalloidin (*green*) (*scale bar*, 20 μm). *F*, EpH4 cells were transfected with a Myc-tagged PATJ expression vector (*top*), a Myc-tagged Par-6A expression vector (*middle*), or a vector that simultaneously produces shRNA against PATJ and expresses GFP (*bottom*). Cells were stained with anti-Myc mAb (*green*) (*top*, *middle*) and RFP-lysenin (*red*) (*scale bar*, 10 μm). *G*, EpH4 cells were transfected with a control H1 promoter vector (*top*) or a vector that produces shRNA against Par-6 (*bottom*). *KD*, knock down. Cells were fixed and stained with RFP-lysenin (*red*) and phalloidin (*green*) (*scale bar*, 10 μm).

Par-6 disrupted the formation of circumferential actin ring. In Par-6-knocked-down cells, apical sphingomyelin clusters were not formed, judging from the staining of RFP-lysenin (Fig. 4*G*). These findings favor the notion that circumferential actin rings, but not TJs, are essential for the establishment of lipid polarity.

Tight Junctions Are Not Diffusion Barriers of Lipids—Next we examined directly whether TJs function as the barrier of lateral diffusion of lipids using fluorescence-labeled lipids. To deliver fluorescence-labeled lipids selectively to the apical membrane, we took advantage of the pH-induced fusion of influenza virus. Influenza virus was labeled with the lipid analog octadecylrhodamine B (R18) as described previously (22). Both wild-type EpH4 cells and ZO-deficient EpH4 cells were incubated with the R18-labeled influenza virus at 4 °C for 30 min. Then the cells were treated with PBS-citrate containing 1 mM $CaCl_2$ and 0.5 mM $MgCl_2$, pH 5.0, to induce viral fusion. We used fluorescence recovery after photobleaching analysis to examine whether or not the R18-labeled influenza virus was efficiently fused with the apical membrane of EpH4 cells. After low pH-triggered fusion of the R18-labeled influenza virus, the apical membrane was photo-bleached, and the subsequent recovery of R18 fluo-

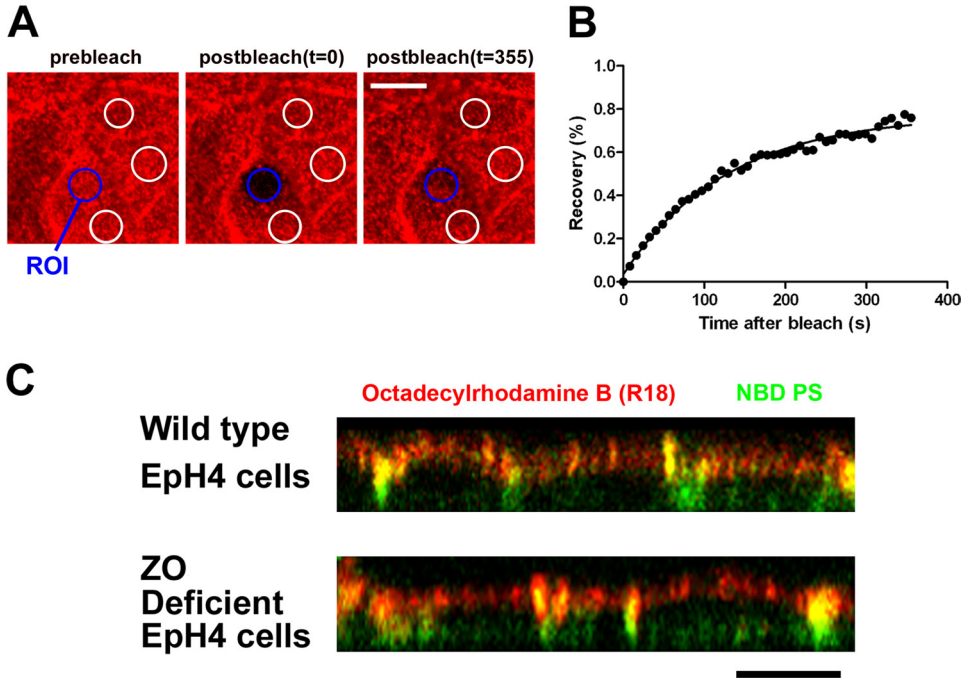

FIGURE 5. **TJs are not essential for the diffusion barrier of lipids in epithelial cells.** *A*, the apical membranes of wild-type EpH4 cells were fused with the R18-labeled influenza virus. The selected region of interest (*blue circle*) was then allowed to recover. The fluorescence intensities of three independent regions that had not been photobleached (*white circles*) were utilized to correct the photo damage (*scale bar*, 10 μm). *ROI*, region of interest. *B*, R18 fluorescence recovery at the apical membrane after photobleaching was calculated as detailed under "Experimental Procedures." The R18 fluorescent lipid inserted into the apical membrane exhibited mobile fractions (fraction value, 73.9 $\pm$ 4.2%). *C*, wild-type EpH4 cells and ZO-deficient EpH4 cells were incubated with the R18-labeled influenza virus (*red*) and NBD-PS (100 μM) (*green*) on ice for 30 min. After the induction of viral fusion, the cells were incubated at 15 °C for 5 min, after which the distributions of R18 and NBD-PS were observed under a confocal microscope. R18 fluorescent lipid (*red*) was retained at the apical membrane even in ZO-deficient EpH4 cells (*scale bar*, 10 μm).

rescence was monitored by time-lapse confocal fluorescence microscopy (Fig. 5*A*). R18 fluorescent lipid inserted into the apical membrane exhibited mobile fractions (fraction value, 73.9% $\pm$ 4.2%), indicating that the R18-labeled influenza virus fused efficiently with the apical membrane and that the R18 fluorescent lipid diffused into the apical membrane (Fig. 5*B*). Then the apical membranes of wild-type EpH4 cells and ZO-deficient EpH4 cells were simultaneously labeled with R18 influenza virus and NBD-PS. NBD-PS underwent a flipping movement and labeled the basolateral membrane and internal membranes in both wild-type EpH4 cells and ZO-deficient EpH4 cells. Interestingly, R18 that was fused with the apical membrane remained at the apical membrane in both wild-type EpH4 cells and ZO-deficient EpH4 cells. These results support the idea that TJs are not diffusion barriers against the lateral diffusion of lipids in epithelial cells (Fig. 5*C*).

DISCUSSION

We have shown that lysenin strongly binds to the membrane domain where sphingomyelin is clustered. Using lysenin as a probe, we demonstrated that clustering of sphingomyelin occurs only in the apical membrane of epithelial cells and that TJs are not essential for the maintenance of lipid polarity. Although TJs have been thought to prevent lipids of the outer leaflet from free diffusion between the apical membrane and basolateral membrane (5), we found that lipids from the apical and basolateral membranes are segregated by a mechanism independent of TJs.

In the previous study, occludin, a four-transmembrane protein at TJs, was reported to be involved in the formation of a diffusion barrier against lipids, because overexpression of a COOH-terminal-truncated mutant of occludin led to impairment of the lipid diffusion barrier in epithelial cells (28). However, Yu *et al.* (29) showed that knockdown of occludin did not affect lipid compartmentalization. Thus, the role of occludin in the barrier formation has remained controversial. Considering that occludin is not concentrated at the boundary of the apical and basolateral membrane domains in ZO-deficient cells as shown in a previous study (11), occludin is unlikely to be involved in the formation of the lipid diffusion barrier.

Other studies have reported that the small GTPases RhoA, Rac1, and Cdc42 were essential for the formation of a lipid diffusion barrier (30, 31). However, the molecular mechanisms by which the small GTPases function in the formation of a lipid diffusion barrier remain to be elucidated.

In other examples of lateral diffusion barriers, septins, a family of cytoskeletal GTPases, were reported to be essential for the compartmentalization of membrane domains (32). In budding yeast, septins localize at the mother-daughter neck and form a diffusion barrier between the mother and daughter cells (33). Septins are conserved from yeast to higher eukaryotes. Recently, septins were shown to localize to the base of the primary cilia at the boundary between the ciliary membrane and apical membrane in epithelial cells (34). Furthermore, knockdown of septin 2 impaired the diffusion barrier at the base of the primary cilium (34). It will be important to examine whether such septin-dependent barriers also exist at the boundary of the

apical membrane and basolateral membrane and prevent free diffusion of lipids.

Complementary to this work, Mostov and co-workers (2) recently showed that when exogenous phosphatidylinositol 3,4,5-trisphosphate (PIP3) (usually localized at the basolateral side in polarized cells) was added to the apical membrane of polarized MDCK cells, PIP3 transformed the membrane protein composition of the apical membrane into a basolateral one, but TJs were not affected, judging from the staining of ZO-1. These results suggest that the formation of TJs and lipid polarity occurs independently in epithelial cells.

In future studies it will be necessary to clarify how the formation of sphingomyelin clusters is regulated as well as the physiological significance of sphingomyelin-cluster formation in the apical membrane and the other mechanisms, *i.e.* those not involving TJs, by which the lateral diffusion of lipids is regulated in epithelial cells.

Acknowledgments—We are indebted to Drs. Ernst Reichmann, Makoto Adachi, Hitoshi Niwa, and Makoto Yamashita for providing reagents. We are also grateful to Dr. Yasuo Mori for kindly allowing us to use the confocal microscope. We thank Akira Kubo for help at the initial phase of this study. J. I. is grateful to So-ichi Ikenouchi for encouragement throughout this work.

REFERENCES

1. Nelson, W. J. (2003) Adaptation of core mechanisms to generate cell polarity. *Nature* **422,** 766–774
2. Gassama-Diagne, A., Yu, W., ter Beest, M., Martin-Belmonte, F., Kierbel, A., Engel, J., and Mostov, K. (2006) Phosphatidylinositol 3,4,5-trisphosphate regulates the formation of the basolateral plasma membrane in epithelial cells. *Nat. Cell Biol.* **8,** 963–970
3. Martin-Belmonte, F., Gassama, A., Datta, A., Yu, W., Rescher, U., Gerke, V., and Mostov, K. (2007) PTEN-mediated apical segregation of phosphoinositides controls epithelial morphogenesis through Cdc42. *Cell* **128,** 383–397
4. van Meer, G., and Simons, K. (1982) Viruses budding from either the apical or the basolateral plasma membrane domain of MDCK cells have unique phospholipid compositions. *EMBO J.* **1,** 847–852
5. van Meer, G., and Simons, K. (1986) The function of tight junctions in maintaining differences in lipid composition between the apical and the basolateral cell surface domains of MDCK cells. *EMBO J.* **5,** 1455–1464
6. Caudron, F., and Barral, Y. (2009) Septins and the lateral compartmentalization of eukaryotic membranes. *Dev. Cell* **16,** 493–506
7. Tsukita, S., Furuse, M., and Itoh, M. (2001) Multifunctional strands in tight junctions. *Nat. Rev. Mol. Cell Biol.* **2,** 285–293
8. Tsukita, S., Katsuno, T., Yamazaki, Y., Umeda, K., and Tamura, A. (2009) Roles of ZO-1 and ZO-2 in establishment of the belt-like adherens and tight junctions with paracellular perm-selective barrier function. *Ann. N.Y. Acad. Sci.* **1165,** 44–52
9. Furuse, M. (2010) Molecular basis of the core structure of tight junctions. *Cold Spring Harb. Perspect. Biol.* **2,** a002907
10. Ikenouchi, J., Furuse, M., Furuse, K., Sasaki, H., and Tsukita, S. (2005) Tricellulin constitutes a novel barrier at tricellular contacts of epithelial cells. *J. Cell Biol.* **171,** 939–945
11. Umeda, K., Ikenouchi, J., Katahira-Tayama, S., Furuse, K., Sasaki, H., Nakayama, M., Matsui, T., Tsukita, S., Furuse, M., and Tsukita, S. (2006) ZO-1 and ZO-2 independently determine where claudins are polymerized in tight-junction strand formation. *Cell* **126,** 741–754
12. Ikenouchi, J., Umeda, K., Tsukita, S., and Furuse, M. (2007) Requirement of ZO-1 for the formation of belt-like adherens junctions during epithelial cell polarization. *J. Cell Biol.* **176,** 779–786
13. Yamazaki, Y., Umeda, K., Wada, M., Nada, S., Okada, M., and Tsukita, S. (2008) ZO-1- and ZO-2-dependent integration of myosin-2 to epithelial zonula adherens. *Mol. Biol. Cell* **19,** 3801–3811
14. Baas, A. F., Kuipers, J., van der Wel, N. N., Batlle, E., Koerten, H. K., Peters, P. J., and Clevers, H. C. (2004) Complete polarization of single intestinal epithelial cells upon activation of LKB1 by STRAD. *Cell* **116,** 457–466
15. Ikenouchi, J., and Umeda, M. (2010) FRMD4A regulates epithelial polarity by connecting Arf6 activation with the PAR complex. *Proc. Natl. Acad. Sci. U.S.A.* **107,** 748–753
16. Kiyokawa, E., Makino, A., Ishii, K., Otsuka, N., Yamaji-Hasegawa, A., and Kobayashi, T. (2004) Recognition of sphingomyelin by lysenin and lysenin-related proteins. *Biochemistry* **43,** 9766–9773
17. Adachi, M., Hamazaki, Y., Kobayashi, Y., Itoh, M., Tsukita, S., and Furuse, M. (2009) Similar and distinct properties of MUPP1 and Patj, two homologous PDZ domain-containing tight-junction proteins. *Mol. Cell. Biol.* **29,** 2372–2389
18. Horger, K. S., Estes, D. J., Capone, R., and Mayer, M. (2009) Films of agarose enable rapid formation of giant liposomes in solutions of physiologic ionic strength. *J. Am. Chem. Soc.* **131,** 1810–1819
19. Carvalho, K., Ramos, L., Roy, C., and Picart, C. (2008) Giant unilamellar vesicles containing phosphatidylinositol 4,5-bisphosphate: characterization and functionality. *Biophys. J.* **95,** 4348–4360
20. Stolz, D. B., Bannish, G., and Jacobson, B. S. (1992) The role of the cytoskeleton and intercellular junctions in the transcellular membrane protein polarity of bovine aortic endothelial cells *in vitro*. *J. Cell Sci.* **103,** 53–68
21. Taguchi, R., Houjou, T., Nakanishi, H., Yamazaki, T., Ishida, M., Imagawa, M., and Shimizu, T. (2005) Focused lipidomics by tandem mass spectrometry. *J. Chromatogr. B Analyt. Technol. Biomed. Life Sci.* **823,** 26–36
22. Lowy, R. J., Sarkar, D. P., Whitnall, M. H., and Blumenthal, R. (1995) Differences in dispersion of influenza virus lipids and proteins during fusion. *Exp. Cell Res.* **216,** 411–421
23. Yamaji, A., Sekizawa, Y., Emoto, K., Sakuraba, H., Inoue, K., Kobayashi, H., and Umeda, M. (1998) Lysenin, a novel sphingomyelin-specific binding protein. *J. Biol. Chem.* **273,** 5300–5306
24. Ishitsuka, R., Yamaji-Hasegawa, A., Makino, A., Hirabayashi, Y., and Kobayashi, T. (2004) A lipid-specific toxin reveals heterogeneity of sphingomyelin-containing membranes. *Biophys. J.* **86,** 296–307
25. Ishitsuka, R., and Kobayashi, T. (2007) Cholesterol and lipid/protein ratio control the oligomerization of a sphingomyelin-specific toxin, lysenin. *Biochemistry* **46,** 1495–1502
26. Veatch, S. L., and Keller, S. L. (2003) Separation of liquid phases in giant vesicles of ternary mixtures of phospholipids and cholesterol. *Biophys. J.* **85,** 3074–3083
27. Pandit, S. A., Jakobsson, E., and Scott, H. L. (2004) Simulation of the early stages of nano-domain formation in mixed bilayers of sphingomyelin, cholesterol, and dioleylphosphatidylcholine. *Biophys. J.* **87,** 3312–3322
28. Balda, M. S., Whitney, J. A., Flores, C., González, S., Cereijido, M., and Matter, K. (1996) Functional dissociation of paracellular permeability and transepithelial electrical resistance and disruption of the apical-basolateral intramembrane diffusion barrier by expression of a mutant tight junction membrane protein. *J. Cell Biol.* **134,** 1031–1049
29. Yu, A. S., McCarthy, K. M., Francis, S. A., McCormack, J. M., Lai, J., Rogers, R. A., Lynch, R. D., and Schneeberger, E. E. (2005) Knockdown of occludin expression leads to diverse phenotypic alterations in epithelial cells. *Am. J. Physiol. Cell Physiol.* **288,** C1231–C1241
30. Jou, T. S., Schneeberger, E. E., and Nelson, W. J. (1998) Structural and functional regulation of tight junctions by RhoA and Rac1 small GTPases. *J. Cell Biol.* **142,** 101–115
31. Rojas, R., Ruiz, W. G., Leung, S. M., Jou, T. S., and Apodaca, G. (2001) Cdc42-dependent modulation of tight junctions and membrane protein traffic in polarized Madin-Darby canine kidney cells. *Mol. Biol. Cell* **12,** 2257–2274
32. Versele, M., and Thorner, J. (2005) Some assembly required. Yeast septins provide the instruction manual. *Trends Cell Biol.* **15,** 414–424
33. Takizawa, P. A., DeRisi, J. L., Wilhelm, J. E., and Vale, R. D. (2000) Plasma membrane compartmentalization in yeast by messenger RNA transport and a septin diffusion barrier. *Science* **290,** 341–344
34. Hu, Q., Milenkovic, L., Jin, H., Scott, M. P., Nachury, M. V., Spiliotis, E. T., and Nelson, W. J. (2010) A septin diffusion barrier at the base of the primary cilium maintains ciliary membrane protein distribution. *Science* **329,** 436–439